Physics Letters B 695 (2011) 82–87

Contents lists available at ScienceDirect

Physics Letters B

www.elsevier.com/locate/physletb

Shape coexistence in odd-mass Au isotopes: Determination of the excitation energy of the lowest intruder state in ^{179}Au

M. Venhart [a,b,*], A.N. Andreyev [a,c], J.L. Wood [d], S. Antalic [e], L. Bianco [f,1], P.T. Greenlees [g], U. Jakobsson [g], P. Jones [g], R. Julin [g], S. Juutinen [g], S. Ketelhut [g], M. Leino [g], M. Nyman [g,2], R.D. Page [f], P. Peura [g], P. Rahkila [g], J. Sarén [g], C. Scholey [g], J. Sorri [g], J. Thomson [f], J. Uusitalo [g]

[a] Instituut voor Kern- en Stralingsfysica, K.U.Leuven, B-3001 Leuven, Belgium
[b] Institute of Physics, Slovak Academy of Sciences, SK-84511 Bratislava, Slovakia
[c] School of Engineering, University of the West of Scotland, Paisley, PA1 2BE, and Scottish Universities Physics Alliance (SUPA), UK
[d] School of Physics, Georgia Institute of Technology, Atlanta, GA 30332-0430, USA
[e] Department of Nuclear Physics and Biophysics, Comenius University, SK-84248 Bratislava, Slovakia
[f] Department of Physics, Oliver Lodge Laboratory, University of Liverpool, Liverpool L69 7ZE, UK
[g] Department of Physics, University of Jyväskylä, FIN-40014 Jyväskylä, Finland

ARTICLE INFO

Article history:
Received 18 June 2010
Received in revised form 30 September 2010
Accepted 25 October 2010
Available online 29 October 2010
Editor: V. Metag

Keywords:
$\pi h_{9/2}^{+1}$ and $\pi f_{7/2}^{+1}$ intruder structures around $N = 104$
Isomer in ^{179}Au

ABSTRACT

Phenomenon of the shape coexistence has been investigated in $^{179}_{79}Au_{100}$. This very neutron-deficient isotope, 18 neutrons away from the stable gold isotope $^{197}_{79}Au_{118}$, was studied by a combination of α-decay and isomer-decay spectroscopy employing the RITU gas-filled separator and the GREAT focal-plane spectrometer at the University of Jyväskylä. A new isomer with $t_{1/2} = 328(2)$ ns was observed and states associated with $\pi d_{3/2}^{-1}$, $\pi s_{1/2}^{-1}$, $\pi f_{7/2}^{+1}$ and $\pi h_{9/2}^{+1}$ structures were revealed. The implications of these results on the systematics of $\pi h_{9/2}^{+1}$ and $\pi f_{7/2}^{+1}$ intruder structures in the odd-mass gold isotopes are discussed. The minimum of the parabolic trend is at $N = 104$, i.e. exactly at the mid-shell point and the $\pi f_{7/2}^{+1}$ structure is dropping in energy relative to the $\pi h_{9/2}^{+1}$ with decreasing mass number.

1. Introduction

A fundamental issue in nuclear structure is the robustness of the closed shells at 2, 8, 20, 28, 50, 82 and 126, which are often referred as magic numbers, as the proton or neutron number takes an extreme value. This is currently under intense investigation because of major advances in experimental accessibility to nuclei very far from stability. Within the past decade, some nuclei that were expected to exhibit the magic properties were found not to be tightly bound [1]. On the other hand, new magic numbers, e.g. $N = 16$ appeared in neutron-rich light nuclei [2,3].

A widely occurring structural feature of nuclei at and near closed shells is intruder states [4–6]. These are states that intrude across closed shells because their energies are dictated not only by shell gaps but also by correlation energies resulting from changing shell occupancies. The occurrence and detailed properties of intruder states need to be thoroughly understood before any conclusions can be made regarding the breakdown of closed shells, which are a pure independent-particle property of nucleons in the nucleus.

The emerging picture of intruder state behavior is one of shape coexisting structures that appear to exhibit an approximately "parabolic" trend in energy [7], often centered near the mid-shell point, e.g., $N = 104$ for nuclei at and near the closed proton shell at $Z = 82$. This particular region is now known to manifest widespread shape coexistence in both odd and even mass isotopes [8–10].

In the past, the intruder states in odd-Au isotopes were the subject of many experiments of different types, see e.g. [11–16] and references therein. However, quantifying the energy trends of these states beyond the neutron mid-shell has proved to be very challenging. Previously, the most relevant data for odd-Au isotopes with $A \leqslant 183$ came from in-beam spectroscopy. There is a further severe difficulty: the states of interest are often isomeric and therefore their decay cannot be detected by in-beam spectrometers. In consequence, most available data are for "floating" bands of states (see, e.g., [11–13]), which give no quantitative information

* Corresponding author.
E-mail address: martin.venhart@fys.kuleuven.be (M. Venhart).
[1] Present address: Department of Physics, University of Guelph, Guelph, Ontario, N1G 2W1, Canada.
[2] Present address: Laboratory of Radiochemistry University of Helsinki, FIN-00014 Helsinki, Finland.

0370-2693
doi:10.1016/j.physletb.2010.10.055

on intruder state energies. A good example is ^{179}Au, where the in-beam γ-ray spectroscopy revealed four rotational bands, but with none of them connected to the ground state [12].

The present Letter reports on results of an experiment carried out to study low-lying intruder states in ^{179}Au ($E_\alpha = 5848$ keV, $t_{1/2} = 7.1$ s [17]). Although ^{179}Au has been known since 1968 [18], experimental information concerning its level structure is still limited, especially at low excitation energies. Hitherto, the low-lying states were studied via the α–γ decay of ^{183}Tl^m [19], but only with the construction of a very incomplete level scheme. In the present study of ^{179}Au the above difficulties are overcome by using combinations of α-decay and isomer-decay spectroscopy together with coincidences between low-energy γ rays and α particles.

2. Experimental details

The experiment was performed at the Accelerator Laboratory of the University of Jyväskylä using the $^{78}\mathrm{Kr} + {}^{107}\mathrm{Ag} \rightarrow {}^{185}\mathrm{Bi}^*$ reaction. A beam of ^{78}Kr^{15+} ions with an average intensity of approximately 90 particle nA was delivered by the K-130 cyclotron and impinged on a target inducing fusion-evaporation reactions. Four bombarding energies of 338, 343, 347 and 352 MeV at the centre of the target were used. Self-supporting metallic targets with a thickness of 700 μg/cm^2 were prepared from isotopically enriched material of ^{107}Ag (98.8% enrichment). To minimize deterioration of the targets, they were mounted on a rotating wheel.

The evaporation residues (ERs) were separated from the primary beam and fission products by the gas-filled recoil separator RITU [20] and implanted into the double-sided silicon strip detector (DSSD) of the focal-plane spectrometer GREAT [21]. Standard correlation techniques between ER implantations and subsequent α decays were employed. K X rays and γ rays were detected by a segmented planar HPGe detector, which was positioned down stream from the DSSDs. The data were collected by a triggerless Total Data Readout acquisition system [22]. A single stream of time-stamped data was analyzed using GRAIN software [23].

3. Experimental results

3.1. Identification of 328(2) ns isomer in ^{179}Au

Nuclei of ^{179}Au were produced directly in $\alpha 2p$ evaporation channel of the above reaction. During the beam time, a total of around 2.6×10^6 ^{179}Au nuclei were implanted into the DSSD. In order to search for γ rays depopulating isomeric states in ^{179}Au, the characteristic α decay was used as a unique tag. Fig. 1(a) depicts a γ-ray singles energy spectrum which was acquired within a time window of 2 μs after ERs were implanted into the DSSD. Only ERs correlated with the α decay of ^{179}Au with a maximum correlation time of 15 s were accepted. The spectrum is dominated by 62.4 and 89.5 keV transitions, which are known deexcitations of states in ^{179}Au [19]. The inset of Fig. 1(a) gives the sum of the time distributions Δt(ER–γ) between ER implantation and subsequent γ ray emission of both prominent transitions seen in the γ-ray singles spectrum. The half-life $t_{1/2} = 328(2)$ ns, was determined by fitting the decay curve with a double-exponential function [24] for the isomeric state which decays by 62.4 and 89.5 keV γ rays.

For more detailed analyses, the data were sorted into an ER–[γ–γ] matrix with Δt(ER–γ) $\leqslant$ 2 μs and $\Delta t(\gamma$–$\gamma) \leqslant 50$ ns conditions. Fig. 1(b) gives a spectrum projected from the γ–γ matrix in coincidence with the 62.4 keV transition. Inspection of Fig. 1(b) shows no evidence for coincidences between the 62.4 and 89.5 keV transitions. This is in disagreement with the level scheme reported in [19], where the 62.4 and 89.5 keV lines are placed in coincidence. Furthermore, a new γ line of 27.1 keV appears in coincidence with the 62.4 keV transition. Moreover 27.1 and 62.4 sum to 89.5, therefore the 89.5 keV γ line is assigned as a parallel transition to a 27.1–62.4 keV cascade.

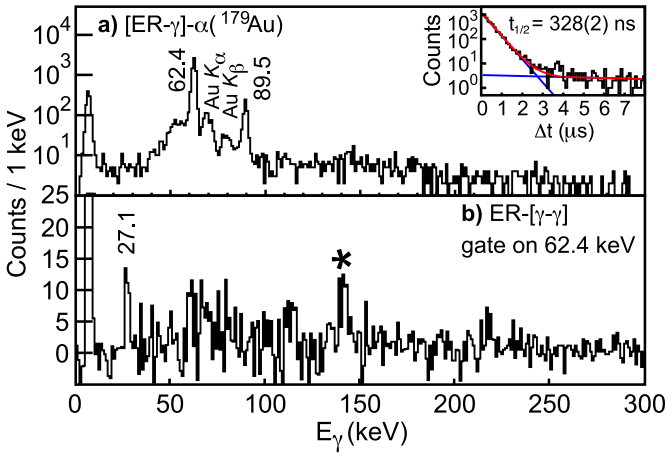

Fig. 1. (Colour online.) (a) Energy spectrum of γ-ray singles of [ER–γ]–α (^{179}Au) events with time conditions of Δt(ER–γ) $\leqslant$ 2 μs and Δt(ER–α) $\leqslant$ 15 s. The inset gives the summed decay curve of the 62.4 and 89.5 keV transitions. The double-exponential fit of the curve is shown by the red line. (b) Spectrum projected from the ER–[γ–γ] matrix with a gate on the 62.4 keV transition. The peak marked with an asterisk is due to beam contamination.

3.2. α decay of ^{183}Tl^m

The excited states of ^{179}Au can also be populated via the α decay of ^{183}Tl^m ($t_{1/2} = 53.3$ ms [19]). In present experiment, nuclei of ^{183}Tl^m were produced via the $2p$ evaporation channel of the $^{78}\mathrm{Kr} + {}^{107}\mathrm{Ag} \rightarrow {}^{185}\mathrm{Bi}^*$ reaction. The studied activity was embedded in the silicon detector, so the measured α spectra suffered from α–e^- summing in the DSSD [25]. As a consequence, peak broadenings or artificial peaks, which can be mistaken for real ones, appear. This effect is significantly reduced in experiments with the sample placed outside of the silicon detector. Therefore, to compare the spectra with and without α–e^- summing, we provide here an α spectrum from our recent experiment at the mass-separator ISOLDE, see Fig. 2(a). In this experiment, to be discussed elsewhere [26], a very clean sample of ^{183}Tl was collected on a thin carbon foil in front of the silicon PIPS detector. The spectrum is dominated by a strong peak with $E_\alpha = 6334(11)$ keV. This value is in agreement with previously reported values [19,27]. We emphasize that due to the specific technique used in the ISOLDE experiment, the α–e^- summing effect is weak. Therefore the 6334 keV peak represents the strongest α-decay peak of ^{183}Tl (see discussion below and Fig. 3). The origins of the additional peak components that lie on the high-energy side of this peak are discussed below.

Fig. 2(b) depicts the two-dimensional ER–[α–γ] spectrum from RITU data with a time condition of $\Delta t(\alpha$–$\gamma) \leqslant 2$ μs. The maximum time for ER–α correlations was 300 ms. Inspection of Fig. 2(b) shows the same 62.4 and 89.5 keV γ rays as were discussed above. Fitting the summed $\Delta t(\alpha$–$\gamma)$ distribution for the two transitions (see the inset of Fig. 2(a)) yielded a half-life of 316(43) ns. The agreement of this value with $t_{1/2} = 328(2)$ ns, deduced above, indicates that the α decay of ^{183}Tl^m feeds the same isomeric state as was identified via direct production of ^{179}Au.

The mass difference $\Delta m = 6586(30)$ keV between the α decaying ^{183}Tl^m and ^{179}Au ground state was calculated using tabulated mass excesses [28,29] and compared with the value of $Q_\alpha = 6479(11)$ keV of the 6334 keV transition. Within experimental uncertainty, the difference between both values, which equals

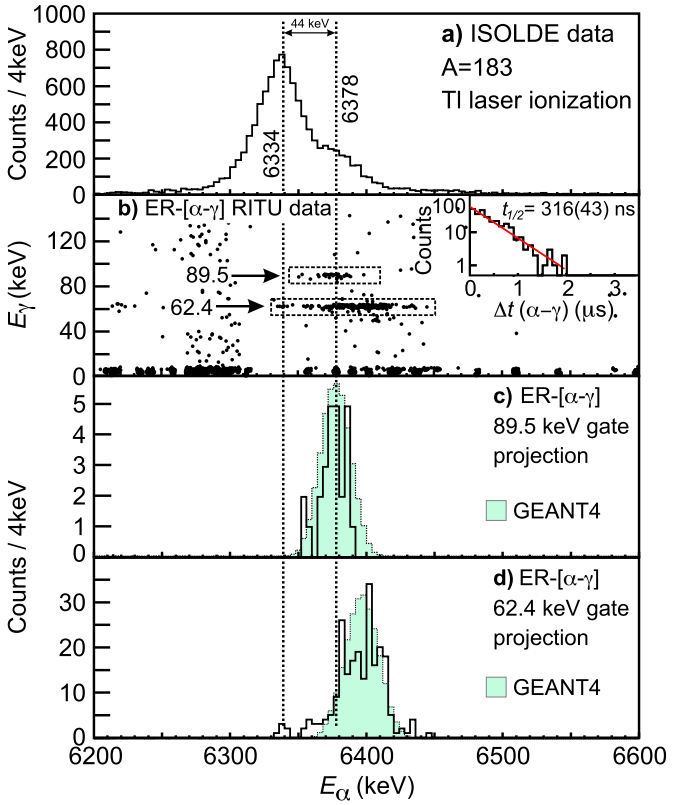

Fig. 2. (Colour online.) (a) α spectrum from ISOLDE experiment, see the text for details. (b) Two-dimensional α–γ spectrum of ER–[α–γ] events from RITU data with Δt(ER–α) $\leqslant$ 300 ms and Δt(ER–γ) $\leqslant$ 2 μs. The inset gives the Δt(α–γ) distribution for events which are denoted by dashed boxes. An exponential fit of the decay curve is shown by the red line. (c) The energy spectrum of α particles coincident with 89.5 keV γ rays. (d) Same as in (c) but in coincidence with 62.4 keV γ rays.

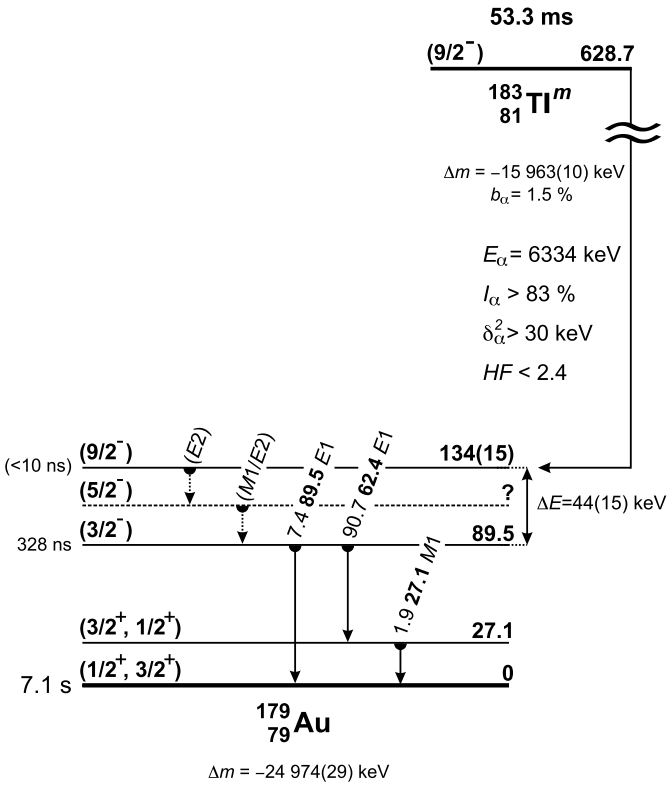

Fig. 3. Partial level scheme of ^{179}Au deduced from the present work. For ^{183}Tl, the values of $t_{1/2}$ and b_α from [30], E_α and I_α from [27] are shown. The hindrance factor, HF was calculated relative to unhindered $0^+ \rightarrow 0^+$ decay of neighboring even–even isotope, ^{182}Hg. The mass excess Δm of ^{179}Au was taken from [29]. The Δm of the ^{183}Tl^m was calculated using the mass excess of ^{183}Tl ground state taken from [28] and the excitation energy of the α-decaying isomer from [26].

107(32) keV leaves room for another transition to be in coincidence with the 89.5 keV line. To elucidate this, the α transitions in coincidence with the γ rays discussed above were studied.

The spectrum of α particles in coincidence with the 89.5 keV transition, which is depicted in Fig. 2(c), shows only a single peak with $E_\alpha = 6378(10)$ keV. The difference of 44(15) keV between $E_\alpha = 6334(11)$ keV measured at ISOLDE is explained by the effect of α–e^- summing in the DSSD. The narrow shape of the spectrum in Fig. 2(c) suggests two or more low-energy transitions follow the 6334 keV α decay, with their energies summing up to 44(15) keV. The scenario with only a single 44(15) keV transition is excluded, as it would create a broadened shape of the spectrum, which is not the case for the present data. On the other hand, if two or more transitions are present, the energy of emitted conversion electrons is reduced and therefore they are easily absorbed in the DSSD with high probability. To lend a weight to this interpretation, full GEANT4 Monte Carlo simulation including atomic relaxation processes (Auger and Coster–Kronig electron emission and X-ray fluorescence) has been performed and the results are given in Fig. 2(c), (d) in light blue. The shape of measured spectrum is well reproduced by the simulation.

As shown above, the 62.4 keV γ line is coincident with the 27.1 keV transition, which undergoes internal conversion with high probability (see Section 3.3). The α–e^- summing effect causes the broadening of the peak as documented in Fig. 2(d). This is well reproduced by GEANT4 simulation.

Above, the difference of 107(32) keV between $\delta m(^{183}\mathrm{Tl}^m - ^{179}\mathrm{Au})$ and Q_α of 6334 keV α decay was determined. Comparison with sum of energies $44(15) + 89.5 = 134(15)$ keV suggests that except the unobserved "44 keV" no other transition is coincident with the 89.5 keV γ line – see proposed level scheme in Fig. 3.

3.3. Multipolarities and partial half-lives of transitions

As a benefit of the high statistics in RITU data, the multipolarities of all three transitions involved in the decay of the 328 ns isomer could be determined unambiguously. The 89.5 keV transition is the only one above the K electron binding energy of Au ($B_K = 80.7$ keV [31]). Thus, the Au K X rays observed in Fig. 1(a) are due to K conversion of the 89.5 keV transition only. An internal conversion coefficient (ICC) for the K atomic shell, from the ratio between K X-ray and 89.5 keV γ-ray intensities, was deduced to be $\alpha_K = 0.48(9)$. This gives an $E1$ multipolarity for the 89.5 keV transition as the theoretical values are $\alpha_K(E1) = 0.44$, $\alpha_K(E2) = 0.68$ and $\alpha_K(M1) = 9.99$ [32]. The total ICC of the 27.1 keV transition was determined by the formula for the number of expected 27.1–62.4 keV γ–γ coincidences:

$$N_{\gamma\gamma} = \frac{N_\gamma(62.4) \times \epsilon(27.1)}{1 + \alpha_{tot}(27.1)},$$

where $N_\gamma(62.4)$ is the number of counts of 62.4 keV γ rays in the singles spectrum and $\epsilon(27.1)$ is the absolute photopeak efficiency of the HPGe detector for 27.1 keV γ rays. Based on the numbers of $N_\gamma(62.4)$ and $N_{\gamma\gamma}$ (see Fig. 1(a), (b)) and taking into account the simulated value of $\epsilon(27.1)$ from [33], a value of $\alpha_{tot} = 72(15)$ for the 27.1 keV transition is obtained. This establishes an $M1$ character for the 27.1 keV transition as theoretically $\alpha_{tot}(E1) = 3$, $\alpha_{tot}(M1) = 60$ and $\alpha_{tot}(E2) = 2557$ [32]. The 62.4 keV transition

Table 1
The transition energies E_γ, intensities I_γ, multipolarities and reduced transition probabilities for γ rays associated with the decay of the 328(2) ns isomer in ^{179}Au.

E_γ (keV)	I_γ (%)	Multipolarity	Reduced transition probability
27.1	1.9(2)	$M1$	–
62.4	90.7(3)	$E1$	$1.88(1) \times 10^{-6}$
89.5	7.4(3)	$E1$	$5.3(2) \times 10^{-8}$

must be parity-changing, because the 62.4–27.1 keV cascade is parallel with the parity-changing 89.5 keV $E1$ transition. Therefore the only possible multipolarity for the 62.4 keV transition is $E1$ as $M2$ and multipoles of higher order are ruled out because of the short half-life of the isomer.

The partial half-life of the 62.4–27.1 keV decay path is 358(3) ns. This rules out the possibility that the 27.1 keV $M1$ transition directly depopulates the isomer. In that case its reduced transition probability, $t_{1/2}(\text{Weisskopf})/t_{1/2}(\text{exp}) = 1.39(1) \times 10^{-6}$ would be inconsistent with known systematics of $M1$ decays [34]. On the other hand, for the 62.4 keV $E1$ transition, the reduced-transition probability of $1.88(1) \times 10^{-6}$ is obtained. This is consistent with experimental values for known delayed $E1$ transitions [34,35]. Therefore it is the 62.4 keV $E1$ transition which deexcites the 328 ns isomer and is followed by a fast 27.1 keV $M1$ transition as shown in Fig. 3. The γ rays associated with the decay of the 328(2) ns isomer in ^{179}Au are summarized in Table 1.

4. Discussion

4.1. $\pi^{+1}(h_{9/2} \oplus f_{7/2})$ intruder structure

Since possible α–e^- summing in the silicon detector is not discussed in Ref. [27], given $I_\alpha = 83\%$ of the strongest α decay needs to be regarded as a lower limit. This gives a reduced α-decay width of $\delta^2_\alpha > 30(7)$ keV, which is calculated for the 6334 keV decay using the Rasmussen prescription with an assumption of $\Delta L = 0$ decay [36]. Relative to $\delta^2_\alpha = 59(4)$ keV for the unhindered α decay of the neighboring even–even isotope ^{182}Hg ($t_{1/2} = 10.83(6)$ s, $E_\alpha = 5867(5)$ keV, $b_\alpha = 15.2(8)\%$ [37]) this gives a hindrance factor $HF < 2.4$, which suggests that the 6334 keV decay is unhindered. As a consequence of this fact and also because of the presumed assignment of $9/2^-$ for ^{183}Tl^m [38], the 134(15) keV state in ^{179}Au, which is fed by the 6334 keV α decay of ^{183}Tl^m, is assigned as $9/2^-$. It is likely that this $9/2^-$ state is a band head of the $\pi h^{+1}_{9/2}$ band, which was discovered in the in-beam experiment [12]. Bands based on $\pi h^{+1}_{9/2}$ and $\pi f^{+1}_{7/2}$ configurations, which are heavily mixed, were reported also in heavier odd-Au isotopes – see, e.g., [13,39] and references therein. Note that the mixed $\pi^{+1}(h_{9/2} \oplus f_{7/2})$ prolate bands in odd-Au isotopes differ from the strongly-coupled oblate bands based on the $9/2^-[514]$ Nilsson orbital, which are known in odd-Tl isotopes [38].

Previously [12,19], based on known systematics of heavier Au isotopes, the ground state of ^{179}Au has been assigned as the $5/2^-$ member of the $\pi h^{+1}_{9/2}$ intruder band. The same state is known to be the ground state of ^{183,185}Au [40,41] and it is interpreted as the odd proton coupled to the 2^+ rotational states of the prolate $2p$–$6h$ ^{182,184}Pt cores. The $5/2^-$ level is a typical example of a rotation-aligned $(j-2)$ state [42,43]. In both ^{183}Au and ^{185}Au, the $5/2^-$ state is located only ∼10 keV below the $9/2^-$ state [14,41]. In the present work, an excitation energy of 134(15) keV was deduced for the $9/2^-$ state. Therefore an $5/2^-$ assignment is unlikely for the ground state of ^{179}Au.

The ground state and first excited state of ^{187,189}Au isotopes are $\pi s^{-1}_{1/2}$ and $\pi d^{-1}_{3/2}$ structures, which are separated by 10 keV (^{189}Au) and 20 keV (^{187}Au) [16]. In $^{181-185}$Au, the intruder structures become the ground state, but the energy difference between the $\pi s^{-1}_{1/2}$ and $\pi d^{-1}_{3/2}$ states remains similar to those in heavier isotopes. The ground state and first excited state of ^{179}Au are connected by an $M1$ transition, which implies $\Delta J = 1$ and no parity change. This is similar to the situation in ^{187,189}Au. Therefore, the ground state and first excited state of ^{179}Au are assigned as $\pi s^{-1}_{1/2}$ and $\pi d^{-1}_{3/2}$ structures. From the present data it is impossible to establish the order of these two states.

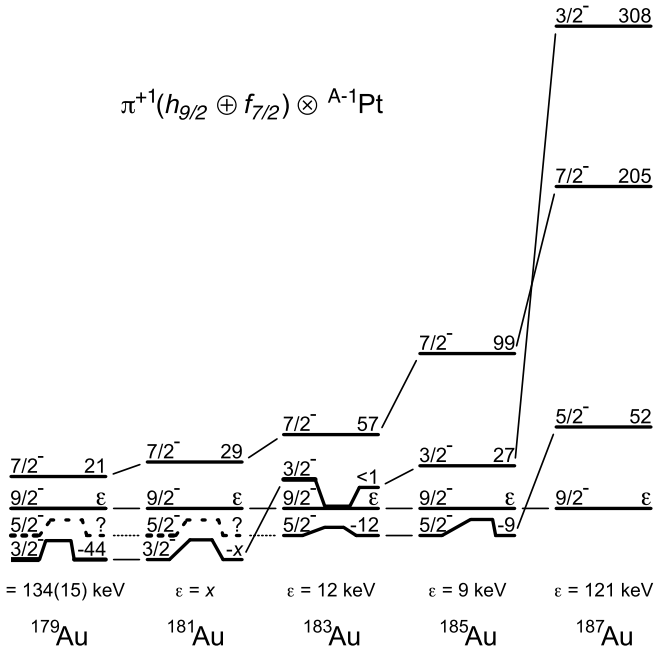

Fig. 4. The band structure of the $\pi^{+1}(h_{9/2} \oplus f_{7/2})$ negative-parity system in $^{179-187}$Au. The excitation energies are given relative to the energy of the $9/2^-$ state, which is denoted as ϵ. The elusive $5/2^-$ states in ^{179,181}Au are indicated with dashed lines. Note that there is no evidence (nor indirect) for the $5/2^-$ state in ^{181}Au, but according to present systematics, it is expected to be localized in close vicinity of the $9/2^-$ level. The data are taken from [12,13,15,40,41].

Only a $1/2^-$ or $3/2^-$ assignment is possible for newly discovered isomer reported here due to the $E1$ character of both transitions which depopulate it, see Fig. 3. Both the $1/2^-$ and $3/2^-$ states are members of a mixed $\pi^{+1}(h_{9/2} \oplus f_{7/2})$ band. According to calculations on the basis of the particle plus triaxial rotor model [44], which were performed in [15], the $1/2^-$ member of the $\pi^{+1}(h_{9/2} \oplus f_{7/2})$ band is expected to be situated above the $3/2^-$ state. Therefore the isomer in ^{179}Au is assigned as the $3/2^-$ state, which is interpreted as the rotation-aligned $(j-2)$ state of the $f_{7/2}$ proton.

The systematics of known $\pi^{+1}(h_{9/2} \oplus f_{7/2})$ bands in odd-A Au isotopes are depicted in Fig. 4. Earlier it was shown that the $3/2^-$ state systematically follows the $7/2^-$ in the $\pi f^{+1}_{7/2}$ band (see Fig. 21 of Ref. [15]), which is very similar to the behavior as a function of deformation of the $5/2^-$ and $9/2^-$ states in the $\pi h^{+1}_{9/2}$ system. Therefore, in the isotope where the $5/2^-$ state is located below the $9/2^-$ state, the $3/2^-$ state can be expected below the $7/2^-$ state. In ^{185}Au, the $3/2^-$ state is 72 keV below the $7/2^-$ state, whereas the $5/2^-$ ground state is only 9 keV below the $9/2^-$ state. A similar situation occurs in ^{183}Au. Since the $\pi f^{+1}_{7/2}$ structure is dropping in energy relative to the $\pi h^{+1}_{9/2}$ structure with decreasing neutron number, see Fig. 4, the $3/2^-$ and $5/2^-$ states cross between ^{183}Au and ^{181}Au, as deduced from the α-decay pattern of ^{181}Au [45]. Prior to the present study no explanation of the change

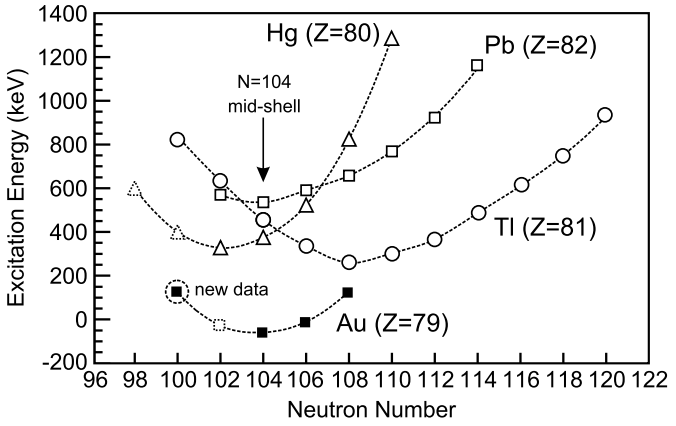

Fig. 5. The systematics of excitation energies of lowest intruder structures in Pb ($Z = 82$), Tl ($Z = 81$), Hg ($Z = 80$) and Au ($Z = 79$) isotopes with even neutron number. The energies of $K^\pi = 0^+$ (Pb and Hg), $9/2^-[514]$ (Tl) and $\pi h^{+1}_{9/2}$ (Au) excited states are given. The energies of $\pi h^{+1}_{9/2}$ structures in odd-Au isotopes are given relative to the $\pi s^{-1}_{1/2}$ state. The excited 0^+ states are not known in ^{178,180}Hg; the given excitation energies were inferred from the structure of the prolate $K^\pi = 0^+$ rotational band [48,49]. No quantitative information on the $\pi h^{+1}_{9/2}$ state in ^{181}Au is available, but it is expected to follow the indicated parabolic trend. The data are taken from Nuclear Data Sheets.

of the ground-state assignment from $5/2^-$ in ^{183,185}Au to $3/2^-$ in ^{181}Au was given. The $3/2^-$ state is also expected to stay below the $5/2^-$ state in ^{179}Au, since the $\pi f^{+1}_{7/2}$ and $\pi h^{+1}_{9/2}$ structures are even closer in ^{181}Au [12]. This supports the $3/2^-$ assignment of the 328(2) ns isomer in ^{179}Au. An extended discussion on the systematics of the $\pi^{+1}(h_{9/2} \oplus f_{7/2})$ bands in odd-A Au and Ir isotopes will be given in forthcoming article [46].

From the present data it is inferred that the $9/2^-$ state decays via two (or more) strongly converted transitions to the $3/2^-$ isomer. This can be explained by the presence of a $5/2^-$ state, which could not be directly observed, situated between the $3/2^-$ isomer and the $9/2^-$ level. The low-energy, in-band $E2$ transitions from the $9/2^-$ to the $5/2^-$ state are known in ^{185}Au [40] and ^{185}Ir [47]. A $B(E2)$ value of ∼200 W.u. was determined in both cases, which clearly demonstrates the collective nature of these transitions. Adopting this $B(E2)$ value for ^{179}Au, a half-life <10 ns is expected for the $9/2^-$ state, which is in agreement with the present data, since an α–e^- summing effect was observed. The elusive $5/2^-$ state would decay via a fast collective $M1/E2$ transition to the $3/2^-$ isomer. Summing in the DSSD of these strongly converted transitions with the 6334 keV α decay does not allow coincidences to be established between this α decay and the γ rays emitted in the decay of the $3/2^-$ isomer. Direct decay of the $9/2^-$ state to $1/2^+$, $3/2^+$ or $3/2^-$ states is excluded as it requires a large change in spin and thus a retarded transition.

4.2. Intruder states in $Z \leqslant 82$ and $N \sim 104$ region

Prior to this study, reliable identification of low-lying structures in the odd-mass Au isotopes was limited to ^{183}Au and heavier isotopes [14,16,15]. In-beam γ-ray spectroscopy has identified floating bands, i.e., bands of unknown excitation energy [11–13], probably built on intruder configurations, but such information does not quantify the excitation energies of the intruder states. The systematics of the $\pi h^{+1}_{9/2}$ in the odd-Au isotopes is depicted in Fig. 5 by the filled squares. The excitation energy is given relative to the $\pi s^{-1}_{1/2}$ structure, which emerges to be constant in odd-mass Au isotopes [16]. The present results for ^{179}Au, together with previously known data for $^{183-187}$Au unambiguously establish that the lowest intruder state in the odd-A Au isotopes reaches a minimum at ^{183}Au, i.e. exactly at the neutron mid-shell point, even in the absence of quantitative information for ^{181}Au. This is important for the global view that intruder states exhibit a parabolic energy pattern with a minimum at or near mid-shell points.

The trend in Au isotopes can be compared with the Hg and Pb isotopes where the intruding, deformed structure (a $K^\pi = 0^+$ band) reaches a minimum energy in ^{182}Hg ($N = 102$) and ^{186}Pb ($N = 104$) [4], see Fig. 5. Also, this trend can be compared with the odd-Tl isotopes where the intruding, deformed structure (a $K^\pi = 9/2^-$ band) reaches a minimum energy in ^{189}Tl ($N = 108$) [50]. This shifting pattern of the parabolic minimum, asymmetry and steepness, combined with evidence of multiple intruder structures [8,14,15], suggests that a very rich spectrum of intruder states remains to be discovered in this mass region and, by implication, in other regions that have been less well studied. Further spectroscopic elucidation of these states is highly demanding. Such experiments should involve unambiguous identification of the $E0$ transitions, which provide model-independent signature of the mixing (and thus repulsion) of configurations with different deformation [51,52].

The quantification of the excitation energies of coexisting intruder structures, particularly their nucleon number dependence, will demand that theory moves beyond mean-field descriptions to quantify the specific nucleon number dependence. Only in this way will we have a reliable framework within which questions of the appearance and disappearance of closed shells can be addressed.

5. Summary

In this Letter a new isomeric state in the neutron-deficient isotope ^{179}Au has been observed for the first time. The high statistics obtained along with the combination of α-decay and isomer spectroscopy, revealed the states associated with the $\pi s^{-1}_{1/2}$, $\pi d^{-1}_{3/2}$ structures and established the excitation energy of $\pi h^{+1}_{9/2}$ and $\pi f^{+1}_{7/2}$ intruder states. The data extend the parabolic trend of the lowest intruder state in Au isotopes ($\pi h^{+1}_{9/2}$) to neutron number $N = 100$. The minimum of the parabolic trend is unambiguously established at $N = 104$. The descent of the $\pi f^{+1}_{7/2}$ structure relative to the $\pi h^{+1}_{9/2}$ structure with decreasing mass number is discussed and it explains the change of the ground-state assignment from $5/2^-$ in ^{183}Au to $3/2^-$ in ^{181}Au. Significant features such as the shifting of the minimum of the intruder parabolic trend in different elements or evolution of the $\pi^{+1}(h_{9/2} \oplus f_{7/2})$ band along odd-Au isotopic chain will require further experimental and theoretical studies.

Acknowledgements

The authors wish to extend their thanks to the technical staff at the Accelerator Laboratory at the University of Jyväskylä for their excellent support. This work has been supported by the Academy of Finland under the Finnish Centre of Excellence Programme (project number 213503), the U.K. Science and Technology Facilities Council, the EU Project EURONS (No. 506065), by the Slovak Grant Agency VEGA (Contract No. 1/0091/10) and by FWO-Vlaanderen (Belgium), GOA/2004/03 (BOF-K.U.Leuven) and the Interuniversity Attraction Poles Programme – Belgian State, Belgian Science Policy (BriX network P6/23). C.S. (contract Nos. 209430) and P.T.G. (contract No. 111965) acknowledge the support of the Academy of Finland. A.N.A. was partially supported by the STFC UK.

References

[1] R.V.F. Janssens, Nature (London) 435 (2005) 897.
[2] A. Ozawa, et al., Phys. Rev. Lett. 84 (2000) 5493.
[3] R. Kanungo, Phys. Rev. Lett. 102 (2009) 152501.
[4] J.L. Wood, W. Heyde, K. Nazarewicz, M. Huyse, P. Van Duppen, Phys. Rep. 215 (1992) 101.
[5] K. Heyde, P. Van Isacker, M. Waroquier, J.L. Wood, R.A. Meyer, Phys. Rep. 102 (1983) 291.
[6] K. Heyde, J.L. Wood, (2010), in preparation.
[7] K. Heyde, Nucl. Phys. A 484 (1988) 275.
[8] A.N. Andreyev, et al., Nature (London) 405 (2000) 430.
[9] R. Julin, K. Helariutta, M. Muikku, J. Phys. G: Nucl. Part. Phys. 27 (2001) R109.
[10] P. Van Duppen, M. Huyse, Hyperfine Interact. 129 (2000) 149.
[11] F.G. Kondev, et al., Phys. Lett. B 512 (2001) 268.
[12] W.F. Mueller, et al., Phys. Rev. C 69 (2004) 064315.
[13] W.F. Mueller, et al., Phys. Rev. C 59 (1999) 2009.
[14] C.D. Papanicolopoulos, et al., Z. Phys. A 330 (1988) 371.
[15] D. Rupnik, et al., Phys. Rev. C 58 (1998) 771.
[16] M.O. Kortelahti, et al., J. Phys. G 14 (1988) 1361.
[17] C.M. Baglin, Nucl. Data Sheets 110 (2009) 265.
[18] A. Siivola, Nucl. Phys. A 109 (1968) 231.
[19] P.M. Raddon, et al., Phys. Rev. C 70 (2004) 064308.
[20] M. Leino, et al., Nucl. Instrum. Methods Phys. Res., Sect. B 99 (1995) 653.
[21] R.D. Page, et al., Nucl. Instrum. Methods Phys. Res., Sect. B 204 (2003) 634.
[22] I.H. Lazarus, et al., IEEE Trans. Nucl. Sci. 48 (2001) 567.
[23] P. Rahkila, Nucl. Instrum. Methods Phys. Res., Sect. A 595 (2008) 637.
[24] M. Leino, S. Yashita, A. Ghiorso, Phys. Rev. C 24 (1981) 2370.
[25] F.P. He, Nucl. Instrum. Methods Phys. Res., Sect. A 274 (1989) 522.
[26] A.N. Andreyev, et al. 2010, private communication.
[27] U.J. Schrewe, et al., Phys. Lett. B 91 (1980) 46.
[28] C. Weber, et al., Nucl. Phys. A 803 (2008) 1.
[29] Y.A. Litvinov, et al., Nucl. Phys. A 756 (2005) 3.
[30] A.N. Andreyev, et al., Phys. Rev. C 73 (2006) 044324.
[31] R. Firestone, V. Shirley, C. Baglin, S. Chu, J. Zipkin, Table of Isotopes, John Wiley & Sons, 1999.
[32] T. Kibédi, Nucl. Instrum. Methods Phys. Res., Sect. A 589 (2008) 202.
[33] A.N. Andreyev, et al., Nucl. Instrum. Methods Phys. Res., Sect. A 533 (2004) 422.
[34] P.M. Endt, At. Data Nucl. Data Tables 26 (1981) 41.
[35] S.V. Rigby, et al., Phys. Rev. C 78 (2008) 034304.
[36] J.O. Rasmussen, Phys. Rev. 113 (1959) 1593.
[37] B. Singh, R.B. Firestone, Nucl. Data Sheets 74 (1995) 383.
[38] M. Muikku, et al., Phys. Rev. C 64 (2001) 044308.
[39] A.J. Larabee, et al., Phys. Lett. B 169 (1986) 21.
[40] K. Wallmeroth, et al., Nucl. Phys. A 493 (1989) 224.
[41] M.I. Macias-Marques, et al., Nucl. Phys. A 427 (1984) 205.
[42] F.S. Stephens, Rev. Mod. Phys. 47 (1975) 43.
[43] J. Meyer-Ter-Vehn, Nucl. Phys. A 249 (1975) 111.
[44] S.F. Larsson, Nucl. Phys. A 307 (1978) 189.
[45] C.R. Bingham, et al., Phys. Rev. C 51 (1985) 125.
[46] M. Venhart, J.L. Wood, (2010), in preparation.
[47] C. Schück, et al., Nucl. Phys. A 325 (1979) 421.
[48] F.G. Kondev, et al., Phys. Rev. C 62 (2000) 044305.
[49] J. Elseviers, M. Venhart, et al., (2010), in preparation.
[50] A.N. Andreyev, et al., Phys. Rev. C 80 (2009) 024302.
[51] K. Heyde, R.A. Meyer, Phys. Rev. C 37 (1988) 2170.
[52] J.L. Wood, et al., Nucl. Phys. A 651 (1999) 323.